Journal of Magnetics 4(2), 39-45 (1999)

Observations of Exchange Coupling in $Nd_2Fe_{14}B/Fe/Nd_2Fe_{14}B$ Sandwich Structures and Their Magnetic Properties

Choong Jin Yang and Sang Won Kim

Eletromagnetic Materials Lab., Research Institute of Industrial Science & Technology(RIST), P.O. Box 135, Pohang 790-330, Korea

(Received 1 January 1999)

Sandwich structures of $Nd_2Fe_{14}B/Fe/Nd_2Fe_{14}B$ magnetic films have been grown by a KrF excimer laser ($\lambda = 248$ nm) ablation technique. Magnetic properties were characterized by varying the thickness of hard ($Nd_2Fe_{14}B$) and soft (Fe) magnetic films and the volume fraction as well. In the (x)nm[NdFeB]/(y)nm[Fe]/(x)nm[NdFeB]/(100)Si structure the thickness (x) was varied from 3.6 to 54 nm, and (y) from 15 to 112 nm. At (y) = 15~20 nm where the volume fraction of Fe corresponded to 61~75%, the sandwich structure exhibited an enhanced M_r/M_s and $_iH_c$ as well from the result of the exchange coupling between the magnetic layers. Experimentally calculated exchange constant (A_s) of $A_s = 2.5\times10^{-10}$ J/m was estimated using the intrinsic coercivity ($_iH_c$) of 1.2 kOe at 5 K for the sandwich magnetic trilayers.

1. Introduction

Recently research work on thin film magnets of NdFeB are of great interest for the applications of monolithic microwave integrated circuit (MMIC), since the film type magnets are essential in biasing the electromagnetic waves through a chip type microwave component [1, 2]. Such film magnets may also become useful in micromechanical devices such as micromotors, actuators and so on [3, 4]. The research works on film magnets initially were started focussing on thick films of SmCo and NdFeB systems having the thickness range of up to 100 μm, which is necessary to obtain a strong enough magnetic flux. At the same time the deposition process employed sputtering techniques [5-8]. However, the substrates used for those film magnets were usually sapphire (Al_2O_3) or MgO wafers which are not practical for those MMIC components. Recently two-dimensional nanoscale NdFeB films emerged as alternative materials. Since the very thin hard magnetic films are concerned for a better understanding of the exchange coupling at the interface of nanodispersed hard and soft magnetic phases in the nanocomposite spring magnets [9-12]. Actually the optimized grain size of each hard ($Nd_2Fe_{14}B$) and soft (Fe) phase and each volume fraction are known to be the key parameters in enhancing the reduced remanence ratio (M_r/M_s) and coercivity as well [13-15].

Mostly the NdFeB thin films were reported to be grown on MgO [16], glass [17, 18]. Also the effect of buffer layers (Cr, Ti) was reported in Cr(or Ti)/NdFeB/Cr(or Ti) multilayers [19]. Recently, some magnetic characteristics of $Nd_2Fe_{14}B$ single layers on Si(100) substrates were reported by the present authors which is useful for a device application [20, 21], and $Fe/Nd_2Fe_{14}B$ layers on grass substrate was also reported [23]. In this study we report the successive work of characterization of $Nd_2Fe_{14}B/Fe/Nd_2Fe_{14}B$ sandwich structures and observations of exchange interaction between the hard/soft magnetic layers.

2. Experimetal Procedures

Film deposition was carried out by pulsation of a KrF excimer laser using a beam energy density of 3.08 J/cm^2. The pulse rate was fixed at 10 Hz with the pulse width of 20 nm. The incident beam was arranged to have 45° with respect to target face, and both the target and substrate heater were kept on rotating at 3 rpm during the deposition. Starting chamber pressure was 4×10^{-6} Torr, and the Si(100) substrate was heated up to the required temperature, 680°C, by an increasing rate of 5°C/min. For the formation of $Nd_2Fe_{14}B$ layers, a target of $Nd_{27.51}Fe_{63.47}B_{9.02}$ composition was used, and pure commercial α-Fe was used for Fe layers. After the deposition was over, the films were cooled down to 300°C at a rate of 3.3°C/min and then cooled to room temperature in the chamber to avoid a possible residual stress. Film thickness was programmed by each laser pulsation and measured using a α-step (Tencor Instrument, Inc.), and then the average value was chosen through three measurements. A vibrating sample magnetometer was used for room temperature measurements, and a SQULD magnetometer was also used for low temperature measurements

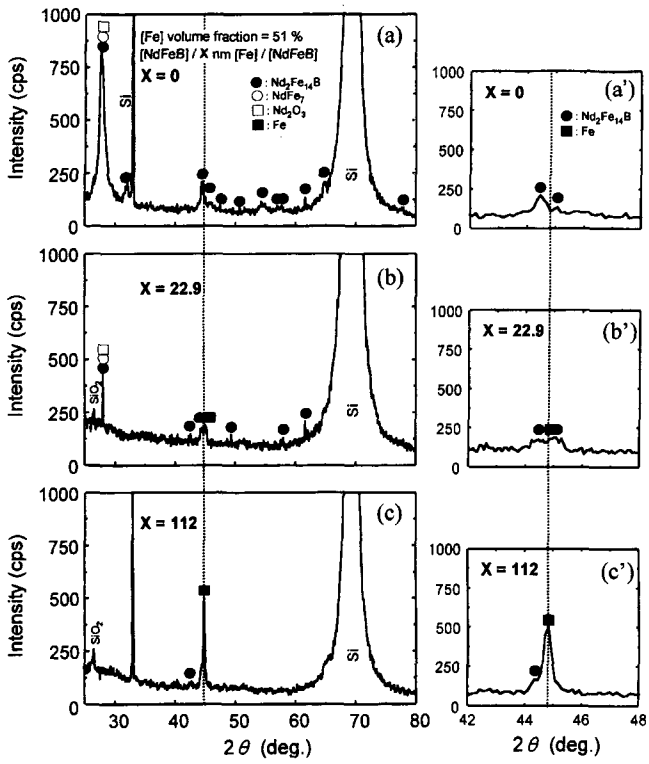

Fig. 1. XRD patterns varying with the [Fe] interlayer's thickness X in [NdFeB]/X nm [Fe]/[NdFeB] trilayers.

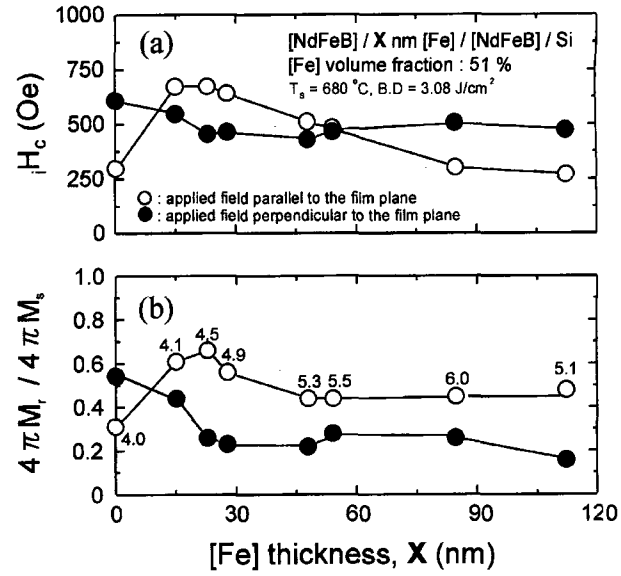

Fig. 2. Dependence of magnetic properties on the [Fe] interlayer's thickness X in [NdFeB]/X nm [Fe]/[NdFeB] trilayers.

from 5~300 K. X-ray diffraction was carried out using a Ni filter to select both the Cu $K_{\alpha 1}$ and Cu $K_{\alpha 2}$ sources. Microstructures of the films were examined by high resolution transmission electron microscopy.

3. Results and Discussion

3.1. Magnetic properties varying with the thickness of Fe and $Nd_2Fe_{14}B$ layers in $Nd_2Fe_{14}B$/Fe/$Nd_2Fe_{14}B$ structure

Initially the thickness (x nm) of Fe layer and its volume fraction were controlled by modeling the sandwich structure such as [$Nd_2Fe_{14}B$]/[Fe]/[$Nd_2Fe_{14}B$]. Fig. 1 shows X-ray diffraction patterns varying with the thickness of Fe layer with a fixed volume fraction, 51%. Accordingly the thickness of $Nd_2Fe_{14}B$ layer was a half of the Fe layer. Basically the $Nd_2Fe_{14}B$ single layer indicates a homogeneous formation of crystallites. As the Fe layer increases from x = 0 through 22.9 to 112 nm, the majority of reflected peaks are observed to be of Fe layer. Since X-rays penetrate through the whole thickness of sandwich layer, those reflected peaks indicate a good measure of volume fraction of each layer. Unfortunately, from the beginning of deposition of the $Nd_2Fe_{14}B$ layer on the Si(100) substrate the formation of Nd_2O_3 was not avoidable as shown in Fig. 1(a). By increasing the thickness of Fe layer the existing oxide is hidden as shown in (b). Along the dashed line which is supposed to be angle of Fe reflection in (a'), (b') and (c'), the overlapped peaks between $Nd_2Fe_{14}B$ and Fe are resolved.

With fixing the volume fraction of Fe layer at 51%, the intrinsic coercivities and M_r/M_s values measured at room temperature are plotted in Fig. 2(a) and (b), respectively. By measuring along the in-plane direction of the trilayer film, enhanced values in ${}_iH_c$ and M_r/M_s=0.7 are observed at a Fe layer's thickness of x = 22.9 nm. In this thickness range, the exchange coupling between the $Nd_2Fe_{14}B$ and Fe layers seems to be activated. In Fig. 2(b) the values of $4\pi M_s$ measured at the corresponding Fe thickness are indicated for each open circle. The $4\pi M_s$ values appeared to increase with increasing the Fe layers thickness from 15 to 112 nm. However, the measured value of $4\pi M_s$ ranged from 4 kG for the $Nd_2Fe_{14}B$ single layer to 5.9 kG for the sandwich of Fe layers thickness of 84 nm which are still low compared with those of bulk composite magnets [10, 11]. Anyway, the $4\pi M_s$ values were found not to vary much above the Fe layers thickness of 48 nm. It is worth noting that the maximum reduced M_r/M_s of 0.84 and ${}_iH_c$ of 3 kOe were obtained in a bulk nanocomposite based on $Nd_2Fe_{14}B$/Fe_3B magnet when the average grain size for both $Nd_2Fe_{14}B$, Fe_3B and Fe was 22 nm [11, 12]. In these film magnets, however, the observed intrinsic coercivity was relatively low which might be due to the formation of rare earth oxide as shown in Fig. 1(a) and (b). Besides since the $Nd_2Fe_{14}B$ layers has the thickness of only 11 nm, the observed $4\pi M_s$ (=4.4 kG) was much lower than a bulk nanocomposite.

$Nd_2Fe_{14}B$ single layers always exhibited the superior magnetic anisotropy along the normal to the film plane [20]. By layering a sandwich structure the anisotropy becomes prominent along the in-plane direction with a higher M_r/M_s rather than along the normal direction. According to the requirement for the application of microwave components the bias magnetic field must be introduced along the in-plane direction of the film magnets. In Fig. 3(a) and (b) the typical hysteresis curves of the sand-

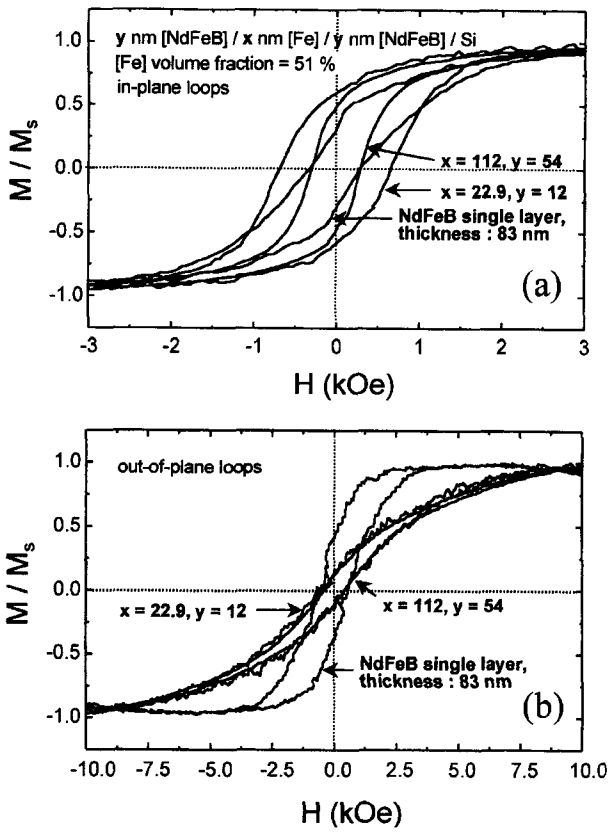

Fig. 3. Hysteresis loops varying with the [Fe] interlayer's thickness X in Y [NdFeB]/X nm [Fe]/[NdFeB] trilayers.

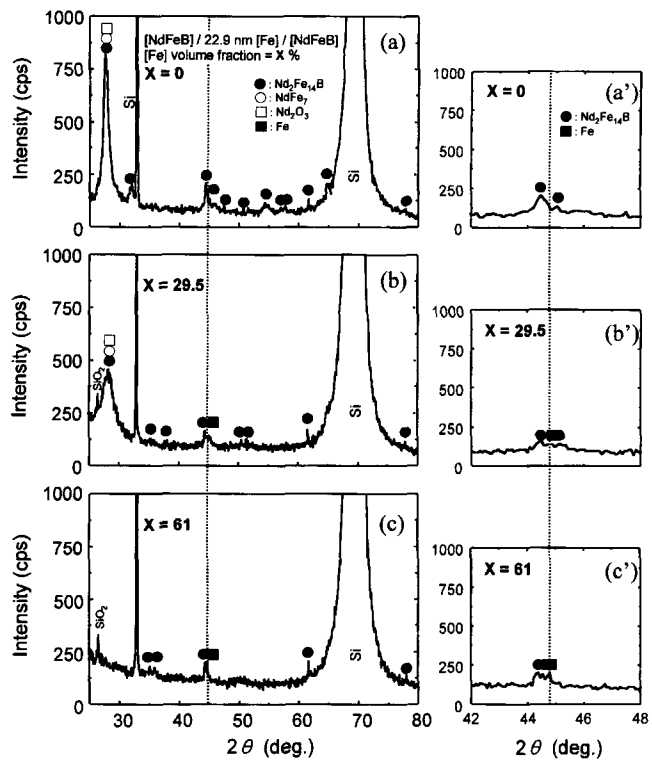

Fig. 4. XRD pattern varying with the [Fe] volume fraction X in [NdFeB]/22.9 nm [Fe]/[NdFeB] trilayers.

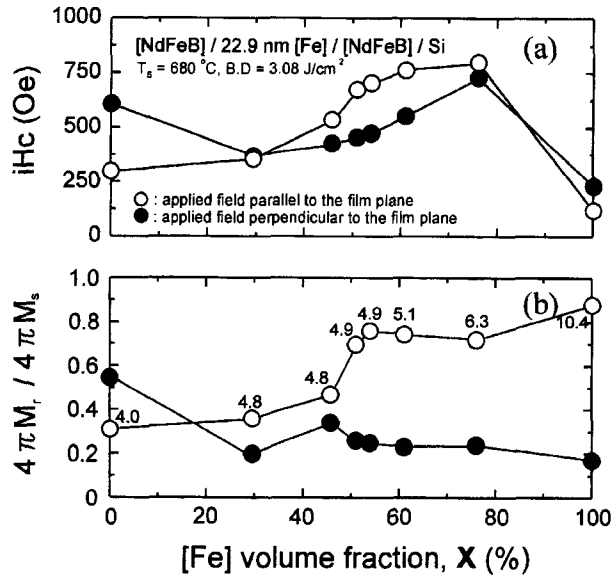

Fig. 5. Dependence of magnetic properties on the [Fe] volume fraction X in [NdFeB]/nm [Fe]/[NdFeB] trilayers.

wich multilayers were plotted by varying the thickness of each $Nd_2Fe_{14}B$ and Fe layer, respectively, with a fixed Fe volume fraction, 51%. For the $Nd_2Fe_{14}B$ single layer the hysteresis curve in Fig. 3(a) exhibits a poor reduced remanence value with an intrinsic coercivity of about 400 Oe. However, when the respective thicknesses of the Fe and $Nd_2Fe_{14}B$ layers are 22.9 and 12 nm, the M_r/M_s value up to 0.7 with an intrinsic coercivity of 750 Oe. Those layers thickness of 22.9 nm (Fe) and 11 nm ($Nd_2Fe_{14}B$) must be an exchange coupling which are exactly the same as reported by Yang *et al.* [10, 11] for a bulk NdFeCoGaHfB nanocomposite magnets. By increasing the both Fe and $Nd_2Fe_{14}B$ layers further, the magnetic properties diminish close to the single layer's characteristics. The hysteresis curves measured along the normal to the film plane in Fig. 3(b) show almost the identical behaviors regardless of the thickness of each layer. Rather the curves of single $Nd_2Fe_{14}B$ layer exhibit a higher reduced remanence value due to the formation of textured structure along the normal direction of the film [16].

Fig. 4(a)~(c') shows X-ray diffraction patterns obtained from the multilayered [$Nd_2Fe_{14}B$]/22.9 nm [Fe]/[$Nd_2Fe_{14}B$]/Si(100) structures varying with the volume fraction of Fe layer from 0 through 29.5% to 61%, respectively. As discussed in Fig. 1, by increasing the thickness of $Nd_2Fe_{14}B$ layer, i.e., decreasing the volume fraction of Fe layer in Fig. (a) and (b), the formation of Nd_2O_3 are shown to be prominent. Upon further decreasing the thickness of $Nd_2Fe_{14}B$ layer the formation of oxide was hidden as shown in (c).

3-2. Magnetic properties varying with the volume fraction of Fe and $Nd_2Fe_{14}B$ layers in $Nd_2Fe_{14}B$/Fe/$Nd_2Fe_{14}B$ sandwich structure

Fig. 5(a) and (b) shows the variations of intrinsic coercivity and M_r/M_s values plotted as a function of volume fraction of Fe layer with fixing the thickness at 22.9 nm.

Therefore increasing the volume fraction of the Fe layer results in reducing the thickness of $Nd_2Fe_{14}B$ layer. Upon further increasing the volume fraction of the Fe layer the coercivity clearly increases up to almost 75% where the thickness of $Nd_2Fe_{14}B$ layer is at most 3.6 nm. It has been already discussed that an exchange coupling might take place at 22.9 nm thickness of Fe layer in this sandwich structure in Fig. 2. The most prominent coupling, therefore, seems to take place at about the volume fraction of 70~80% of Fe layer as shown in Fig. 5(a). At this range the intrinsic coercivity of $Nd_2Fe_{14}B/Fe/Nd_2Fe_{14}B$ sandwich structures exhibits the higher values than that of $Nd_2Fe_{14}B$ single layer and that of Fe single layer as well. At these ranges of volume fraction in Fig. 4(c), the M_r/M_s values are also shown to be enhanced to about 0.7~0.8 which are quite high for hard magnetic thin films. It is worth noting that this exchange coupling between the Fe and $Nd_2Fe_{14}B$ layers would not take place when the volume fraction of magnetically soft Fe layer is under 50%. From the advent of bulk nanocomposite magnets based on $Nd_2Fe_{14}B/Fe$ or $Nd_2Fe_{14}B/Fe_3B$, Kneller *et al.* [13] simulated the volume fraction of Fe to be about 90% when the exchange coupling might take place, while recent report by Fukunaga's simulation [22] estimated that the coupling would be most prominent when the volume fraction of Fe phase is about 65% with the grain size of 20 nm. Therefore the experimental result of the present study is quite reasonable and reliable on the basis of those predictions. In Fig. 5(b) the M_r/M_s value of the Fe single layer, i.e., when the volume fraction of Fe is 100%, is almost 0.9. However, this value is nothing to do with the exchange coupling but due to the occurrence of soft magnetic properties of Fe layer. The relatively low M_r/M_s values observed along the normal direction to the plane in Fig. 5(b) seem to be due to the extremely small volume fraction of the $Nd_2Fe_{14}B$ layers.

Fig. 6(a) and (b) shows the typical hysteresis curves of $[Nd_2Fe_{14}B]$/22.9 nm [Fe]/$[Nd_2Fe_{14}B]$/Si(100) sandwich multilayers varying the volume fraction of Fe layer. The measured values of $4\pi M_s$ also are denoted at each corresponding Fe volume fraction. For the Fe volume fraction up to 29.5% in Fig. 6(a), no exchange coupling seems to take place indicated by the low coercivity and M_r/M_s as well. By increasing the Fe volume up to 61%, however, the M_r/M_s value is enhanced to 0.7 with a high coercivity value around 1 kOe even the thickness of the $Nd_2Fe_{14}B$ layer is only 7.3 nm. For the same reason, the hysteresis curves measured along the normal direction to the film plane show the almost identical coercivity when the volume fraction of the Fe layer is below 30% as shown in Fig. 6(b). Rather the M_r/M_s for the single $Nd_2Fe_{14}B$ layer is high due to the fact that

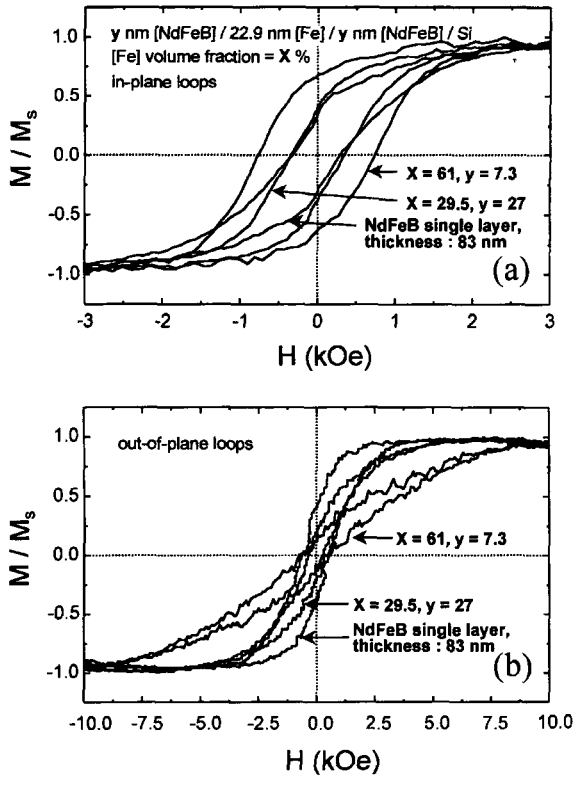

Fig. 6. Hysteresis loops varying with the [Fe] volume fraction X in Y nm [NdFeB]/22.9 nm [Fe]/Y nm [NdFeB] trilayers.

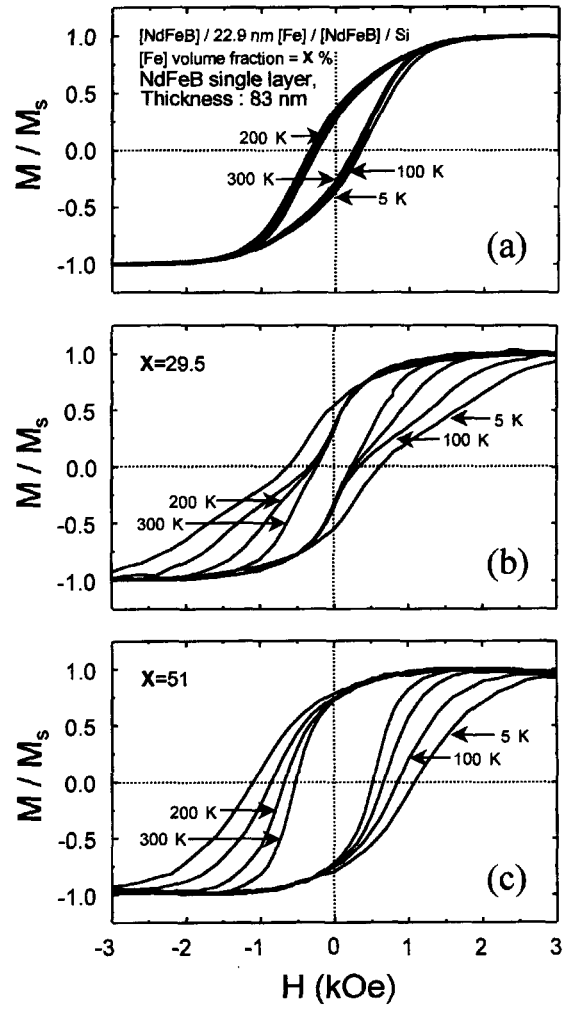

Fig. 7. The typical hysreresis loops measured at low temperature.

a textured structure normal to the film plane has developed [19-21].

The hysteresis curves at low temperatures of $Nd_2Fe_{14}B$/ 22.9 nm [Fe]/[$Nd_2Fe_{14}B$] with varying the volume fraction of Fe layer are demonstrated in Fig. 7(a)-(c), For the $Nd_2Fe_{14}B$ single layer no changes in the hysteresis curves can be seen with lowering the temperature from 300 K to 5 K. Upon increasing the volume fraction of Fe layer to 29.5 % in Fig. 7(b) when the thickness of $Nd_2Fe_{14}B$ layer is almost 30 nm, a weak exchange begins to take place at 5 K. By increasing the volume fraction of Fe layer further to 51%, however, exchange coupling becomes prominent with

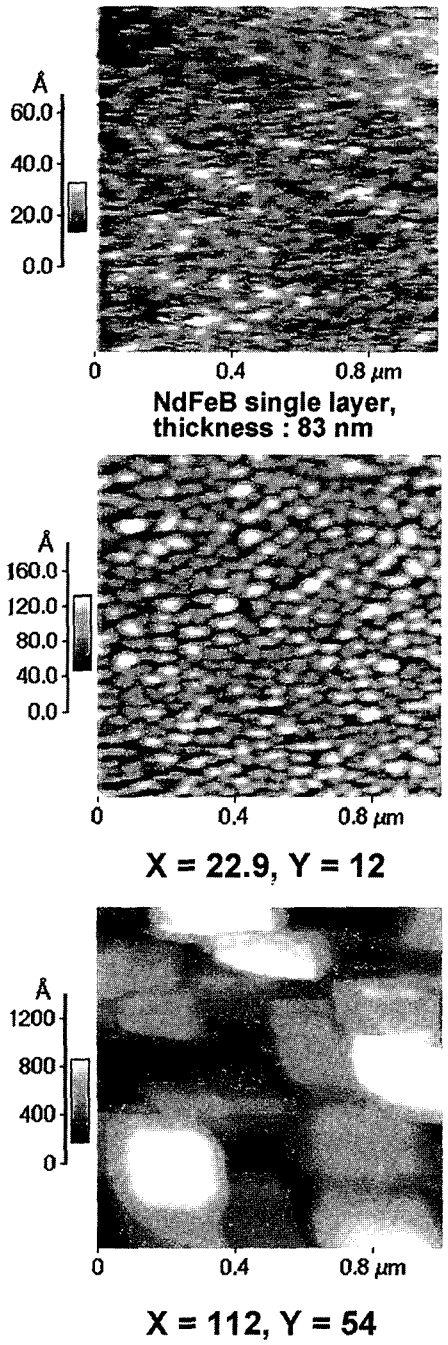

Fig. 8. AFM images varying with the [Fe] interlayers thickness X in Y nm [NdFeB]/X nm [Fe]/Y nm [NdFeB] trilayers.

lowering the temperature as shown in Fig. 7(c). By a strong coupling the intrinsic coercivity of $Nd_2Fe_{14}B$/Fe/$Nd_2Fe_{14}B$ trilayer increases such as 0.6 → 0.75 → 0.9 → 1.2 kOe as the measured temperature decreases from 300 K to 200 → 100 → 5 K. The calculation resulted in a $d_iH_c(T)/dT$ =-0.24 %/K.

As suggested by Kneller and Hawig [13], the critical thickness (tcs) of soft magnetic layer (Fe) is estimated by:

$$t_{cs} = 2(A_s/2K_h)^{1/2}$$

and, when the soft and hard magnetic phase are supposed to have the same thickness, the coercivity of the nanocomposite (H_c) is given by:

$$H_c = \frac{A_s \pi^2}{2M_s} \frac{1}{t_{cs}^2}$$

where A_s is the exchange constant of the soft phase, K_h is the anisotropy constant of hard phase, and M_s is the saturation magnetic moment of the soft phase, respectively. Employing the measured Fe layer's thickness in this study (22.9 nm), and by quoting K_h=9.4×10^6 J/m^3 [9], the exchange constant A_s=2.5×10^{-10} J/m which is quite large (almost order of one) compared with other bulk magnetic materials can be estimated. As shown in Fig. 7(c), the intrinsic coercivity at 5 K was found to be 1.2 kOe. If this coercivity is supposed to be merely from the exchange force, then the coercivity value of 1.2 kOe for these nanocomposite multilayers is too small taking into account that the exchange constant, A_s=2.5×10^{-10} J/m results in $_iH_c$=5.02 kOe.

3-3. Microstructure of the sandwich $Nd_2Fe_{14}B$/Fe/ $Nd_2Fe_{14}B$/Si(100) trilayers

Fig. 8 shows atomic force microscopic images displaying the surface aspect of the $Nd_2Fe_{14}B$/Fe/$Nd_2Fe_{14}B$/Si(100) trilayers. X indicates the Fe layer's thickness and Y for the thickness of $Nd_2Fe_{14}B$ layers. Fixing the volume fraction of Fe layer at 51%, the particle size of outer layer, i.e., $Nd_2Fe_{14}B$ layer, are shown to be increased proportional to the thickness of Fe layer. Actually it is not clear if the particles shown in the figures are grains or not even though we believe that the particles may be the grains. The electron microscopy work on the sandwich structure was not successful to distinguish the grains of each layer. For $Nd_2Fe_{14}B$ single layer with the thickness up to 83 nm, the surface looks very smooth. However, once Fe interlayer has been deposited under $Nd_2Fe_{14}B$ layer, the final particle aspect of the outer $Nd_2Fe_{14}B$ layer tends to grow very rapidly according to the duration of ablation time of Fe layer even though the thickness of $Nd_2Fe_{14}B$ layer is thin enough comparing with Fe layer's. This was also true for the same sandwich structure with fixing the Fe layer's thickness at 22.9 nm but varying the volume fraction of Fe layer, i.e., decreasing the thickness of $Nd_2Fe_{14}B$ layers as shown in Fig. 9. The fig-

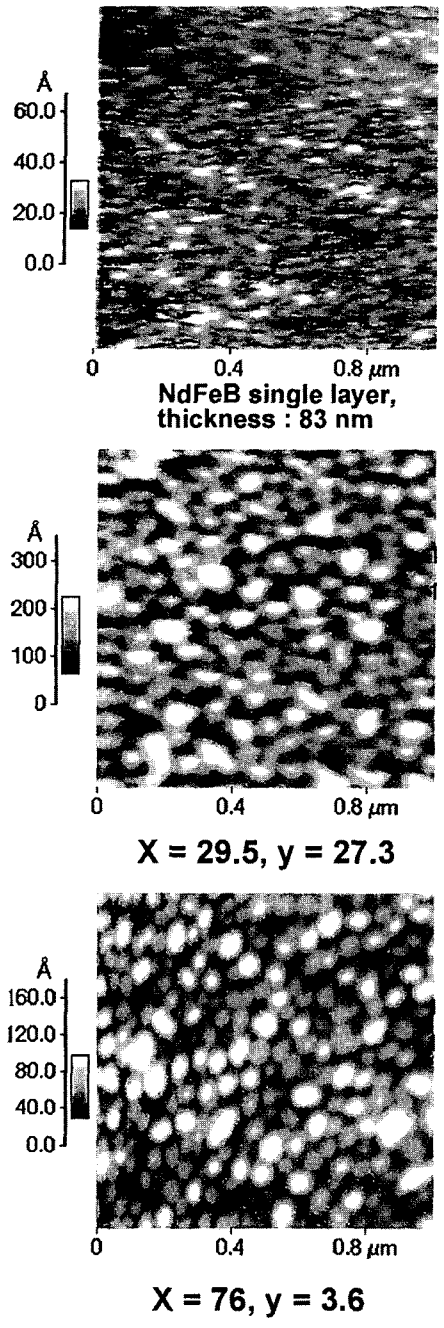

Fig. 9. AFM images varying with the [Fe] volume fraction X in Y nm [NdFeB]/22.9 nm [Fe]/Y nm [NdFeB] trilayers.

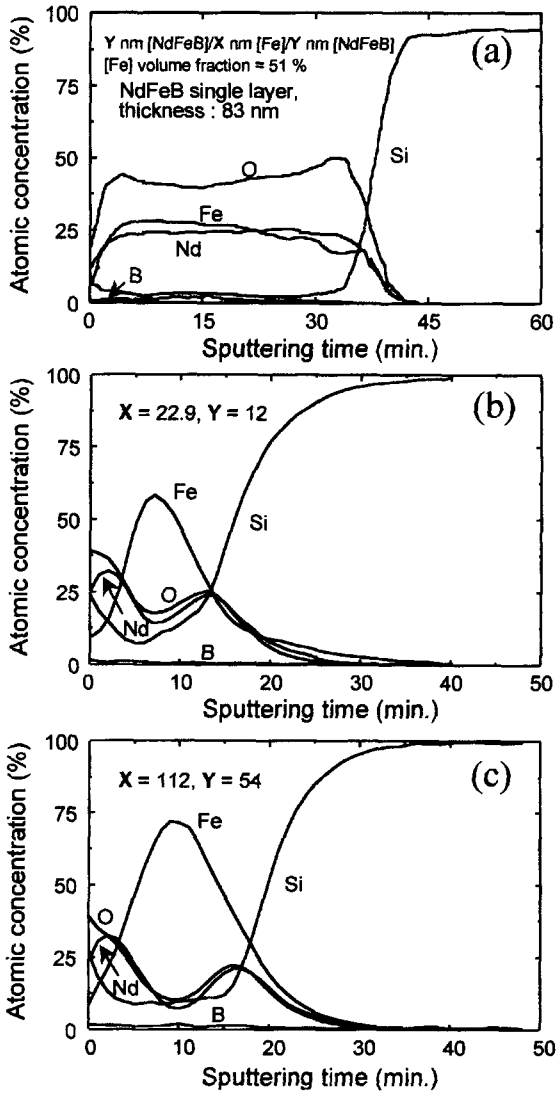

Fig. 10. Auger depth profiles varying with the [Fe] interlayers thickness X in Y nm [NdFeB]/X nm [Fe]/Y nm [NdFeB].

ures show the grain aspects of the outer $Nd_2Fe_{14}B$ layers followed by Fe layers grown in different volume fraction such as 29.5% and 76% as well. The [Fe] layers thickness of 22.9 nm resulted in the outer $Nd_2Fe_{14}B$ of particles of about 3.5~4.5 nm which is much finer than those of the sandwich films with the [Fe] layers thickness of 112 nm as shown in Fig. 8. Accordingly even if the particle aspect of the outer $Nd_2Fe_{14}B$ layer tend to be influenced critically by the previous deposition history of Fe layer, the [Fe] layers thickness of 29~76 nm seems to give a very smooth and fine particles of the following $Nd_2Fe_{14}B$ layer.

As mentioned earlier, a deterioration in the magnetic properties of these multilayers seems to be the formation of Nd oxide and the diffusion of Si into magnetic layer. Some details of Auger surface analysis were made as shown in Fig. 11(a)~(c). Although these Auger analysis curves do not indicate an exact atomic concentration the profiles of each atom demonstrate the general trend corresponding to the built layer. From the beginning of layering up, the Nd oxide are shown to form indicated by the identical concentration profiles between Nd and oxygen. Continuing the ablation an active diffusion of Si into the magnetic layers can be seen to take place as shown in Fig. 11(b) and (c).

4. Conclusion

A KrF excimer laser ablation was employed for the deposition of $Nd_2Fe_{14}B$/Fe/$Nd_2Fe_{14}B$ sandwich structured films on (100)Si wafer. The magnetic properties of those films were characterized varying the thickness and volume of each magnetic layer. A good evidence of an exchange cou-

pling between those magnetic layers were observed when the thickness of Fe layer was 15~20 nm with the volume fraction of 61~75%. At this condition an exchange constant (A_s) of $A_s=2.5\times10^{-10}$ J/m was calculated using the observed intrinsic coercivity 1.2 kOe at 5 K. This estimated exchange constant seems to be quite a large number compared with other bulk magnetic materials.

The authors are thankful for the support and grant by The Korean Ministry of Science & Technology under Contract No 97E007.

References

[1] D. D. Stancil, Microw. Opt. Technology Lett., **2**, 53 (1989).
[2] M. Levy, R. M. Osgodd, F. J. Cadieu and R. Wolfe, IEEE Photonic Technol. Lett., **8**, 903 (1996).
[3] S. Yamashida, J. Yamasaki and N. Iwabuchi, J. Appl. Phys., **70**, 6627 (1991).
[4] H. Lemke, T. Lang and C. Heiden, J. Magn. Magn. Mater., **148**, 426 (1995).
[5] F. J. Cadieu, T. D. Cheung and L. Wickramasekara, J. Magn. Magn. Mater., **54-57**, 535 (1986).
[6] F. J. Cadieu, J. Appl. Phys., **61** (1987) 4105.
[7] Y. Okumura, H. Fusimori, O. Suzuki and H. Moria, IEEE Trans, Magn., **MAG-30**, 4038 (1994).
[8] A. Kapitanov, N. V. Kornilov and V. Yu. Tsvetkov, **127**, 289 (1993).
[9] R. Coehoorn, D. B. De Mooji and C. De Waard, J. Magn. Magn. Mater., **80**, 101 (1989).
[10] C. J. Yang and E. B. Park, J. Magn. Magn. Mater., **166**(2), 243 (1996).
[11] C. J. Yang and E. B. Park, J. Magn. Magn. Mater., **168**, 278 (1997).
[12] Youhui Gao, C. J. Yang and E. B. Park, J. Magn. Magn. Mater., **186**, 97 (1998).
[13] E. F. Kneller and R. Hawig, IEEE Trans, Mag., **MAG-27**, 3588 (1991).
[14] T. Schrefl, J. Fidler and H. Kronmuller, Phys. Rev., **B49**, 6100 (1994).
[15] R. Skomski and J. M. D. Coey, IEEE Trans. Mag., **MAG-29**(6), 2860 (1993).
[16] D. J. Keavney, E. E. Fullerton and S. D. Bader, J. Appl. Phys., **81**(8), 4441 (1997).
[17] S. Parhofer, G. Gieres, J. Wecker and L. Schultz, J. Magn. Magn. Mater., **163**, 32 (1996).
[18] S. Parhofer, C. Kuhrt, J. Wecker and L. Schultz, J. Appl. Phys., **83**, 2735 (1998).
[19] T. Shima, A. Kamegawa and H. Fujimori, J. Magn. Magn. Mater., **177-181**, 911 (1998).
[20] C. J. Yang and S. W. Kim, J. Appl. Phys., **83**(11), 6620 (1998).
[21] C. J. Yang and S. W. Kim, J. Magn. Magn. Mater., **188**, 100 (1998).
[22] J. Kuma, N. Kitajima and H. Fukunaga, J. Appl. Phys., **83**(11), 6623 (1998).
[23] M. Shindo, M. Ishizone, H. Kato and A. Sakuma, J. Magn. Magn. Mater., **161**, L1 (1996).